

A critical study on the experimental determination of stiffness and viscosity of the human triceps surae by free vibration methods

Proc IMechE Part H:
J Engineering in Medicine
227(9) 935–954
© IMechE 2013
Reprints and permissions:
sagepub.co.uk/journalsPermissions.nav
DOI: 10.1177/0954411913487851
pjh.sagepub.com


Federico París-García¹, Alberto Barroso², José Cañas², Juan Ribas³ and Federico París²

Abstract

Muscles and tendons play an important role in human performance. Their mechanical behaviour can be described by analytical/numerical models including springs and dampers. Free vibration techniques are a widely used approach to the in vivo determination of stiffness and viscosity of muscle–tendon complexes involved in sport movements. By considering the data reported in the literature, it appears that the visco-elastic properties of the triceps surae muscle–tendon complexes are independent of the modality in which free vibration is induced as well as they do not depend on the composition of the population of subjects submitted to the experiments. This research will critically discuss this important aspect focussing in particular on two studies documented in the literature. For this purpose, two equipments will be developed to reproduce literature experiments under the assumption that the oscillating part of the body behaves as a single-degree-of-freedom system: The governing degree of freedom is associated with the vertical displacement of the lower leg or with the rotation of the foot around the ankle articulation. Unlike literature, measurements are now conducted on the same population of subjects in order to draw more general conclusions on the real equivalence of results and validity of the mechanical properties determined experimentally. Free vibration tests are accurately simulated by analytical models describing the response of each vibrating system. It is found that if the two measurement protocols are applied to the same population of individuals as it is done in this study, values of visco-elastic properties of muscle–tendon complexes extracted from experimental data are significantly different, the differences presenting a convincing consistency. This result is in contrast with the literature and confirms the need to evaluate results of free vibration techniques by taking homogeneous bases of comparison.

Keywords

Visco-elastic properties of human triceps surae, in vivo measurements, free vibration techniques, data fitting

Date received: 26 September 2012; accepted: 28 March 2013

Introduction

Muscular and tendinous fibres play an important role in improving human performance. Since mechanical behaviour of muscles and tendons resembles a visco-elastic spring, their response can be described by simple elastic models including spring and damper elements.¹

Stretch-shortening cycles (SSC) appear in many movements performed by the human body. The muscle–tendon complex (MTC) can work in the following three different ways:^{2,3} (1) eccentrically (the muscle opposes elongation), (2) isometrically (there is neither stretching nor shortening of the muscle) and (3) concentrically (there is a shortening of the muscle). The global mechanical response of MTC depends

essentially on the following two factors: (1) transformation of chemical energy into mechanical energy (i.e. muscular shortening); and (2) efficiency of MTC elastic components in terms of their capacity to store elastic energy at the macroscopic level in the tendons and at the microscopic level in the muscles by means of titin,

¹Faculty of Sport Science, University of Pablo de Olavide, Seville, Spain

²School of Engineering, University of Seville, Seville, Spain

³Faculty of Medicine, University of Seville, Seville, Spain

Corresponding author:

Alberto Barroso, School of Engineering, University of Seville, Seville, E-41092, Spain.

Email: abc@etsi.us.es

which is the elastic protein incorporated in the sarcomere that is in turn the smallest functional part of a muscle.⁴

In order to establish a direct relationship between the elastic parameters of an MTC (typically stiffness and damping) and its corresponding efficiency in a particular sport discipline, the MTC must play an important role in the development of the movements entailed by the discipline in question. For example, the triceps surae (TS), formed by the gastrocnemius (the muscle that generates movement), the soleus (the postural muscle) and the Achilles tendon, is the MTC that permits plantar flexion, a basic phase in the biomechanics of walking.⁴ Therefore, the TS is of fundamental importance in all sport disciplines involving general displacements.

Experimental determination of MTC visco-elastic characteristics is widely documented in the literature. There are two possible approaches to solve this problem as follows: (1) protocols based on the use of cadavers such as the quick-release method,⁵ the α -method⁶ and the null-point method⁷ and (2) protocols based on in vivo measurements such as the quick-release method,^{8,9} application of ultrasounds¹⁰ and free vibration techniques.^{1,11–14}

The basic idea behind free vibration techniques that appear to be the approach most commonly used in the literature is to induce damped free vibrations in the region of investigation by perturbing through impact another part of the human body. Some characteristic parameter describing the free vibration movement (typically a force) is experimentally measured and then related by a theoretical/analytical/numerical model to visco-elastic properties of tendons and muscles involved in the movement. If free vibration techniques are utilized, it is however necessary to check that experimental measurements are in good agreement with the theoretical predictions provided by models within the limits of validity of each assumption made in the modelling stage.

From a careful survey of the literature, it might appear that visco-elastic properties of the human TS MTC be independent of the modality in which free vibration occurs as well as they do not depend on the composition of the population of subjects submitted to experiments. For example, Fukashiro et al.¹² and Babic and Lenarcic¹³ considered different vibration movements: the displacement of the lower leg¹² and the rotation of the foot around the ankle articulation,¹³ respectively. Although Fukashiro et al.¹² and Babic and Lenarcic¹³ followed the same general principle (i.e. free vibration of the MTC under investigation), the movements monitored in the experimental measurements and, consequently, the associated dynamic equations are completely different and involve different auxiliary muscular resorts. Furthermore, experiments were carried out on unrelated sets of people. However, visco-elastic properties were found to be quite similar.

In view of this, this study will critically review the determination of TS visco-elastic parameters documented in the previous studies.^{12,13} The present investigation is motivated by the fact that although the procedures developed in the previous studies^{12,13} are derived from strong theoretical foundations, the similarity between the results obtained does not seem to have a physical explanation. Therefore, it may be very useful to assess in much deeper detail the real significance of the measured values. Hence, the main objective of this article is to assess the true generality and representativity of each procedure in itself as well as to critically compare results. For this purpose, measurements described in the previous studies^{12,13} are reproduced in this research by implementing two experimental set-ups able to carry out the tests. Unlike literature, experimental protocols are carried out on the same population of individuals to avoid further uncertainties in the interpretation of the results.

It is found that visco-elastic properties of the human TS MTC extracted from experimental data are now significantly different. The differences found present a convincing consistency. This result is in contrast with the literature data and confirms the need to evaluate results of free vibration techniques by considering homogeneous bases of comparison.

This article is structured as follows: The 'Determination of visco-elastic properties of the human TS MTC' section describes the free vibration experimental set-ups, the corresponding theoretical models to simulate dynamic behaviour and the least-square approach used to extract TS visco-elastic properties; the 'Results and discussion' section presents and discusses experimental results in terms of stiffness and viscosity; and finally, the 'Conclusions' section summarizes the main findings of this study.

Determination of visco-elastic properties of the human TS MTC

In this research, visco-elastic properties of the human TS were determined by conducting in vivo measurements. For this purpose, two experimental set-ups implementing the free vibration approach were specifically designed and realized. As mentioned previously, the rationale behind free vibration techniques is to originate a free damped vibration of an isolated part of the body. In this case, the vibration response was controlled by the visco-elastic properties of the TS (Achilles tendon + soleus + gastrocnemius) complex that is assumed to behave as a 1-degree-of-freedom dynamic system.

The global reaction force developed in the oscillation period was monitored by a load cell and the force values measured over the vibration period were compared with their counterpart predicted by a theoretical model reproducing the 1-degree-of-freedom dynamic system assumed. In this way, it is possible to build an

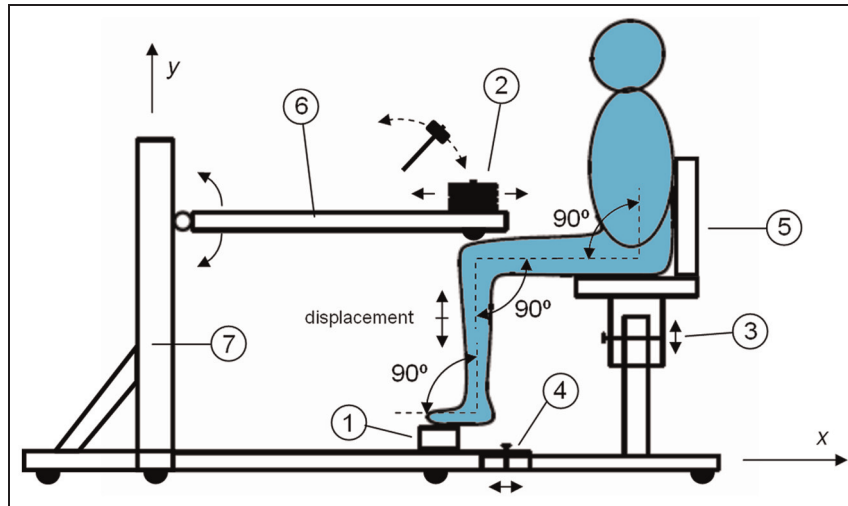


Figure 1. Schematic diagram of the experimental set-up for determining TS visco-elastic properties based on the vertical displacement of the lower leg.

error function depending on the unknown visco-elastic properties of TS. Finally, stiffness and damping constants can be determined via least-square fitting of experimental data. The experimental equipments, the corresponding theoretical models and the least-square fitting procedure are described in detail in the rest of this section.

TS identification procedure based on the vertical displacement of the lower leg

The experimental apparatus was designed following the measurement approach described in the study by Fukushima et al.¹² The basic idea is to generate a configuration of the human body by allowing a vertical displacement in the lower leg, which will be used as the reference equation of motion. This vertical displacement will be accompanied by rotations of the foot and of the upper leg. The overview schematic diagram of the testing apparatus is shown in Figure 1. Since the frontal part of the foot is simply supported by a plate, the vertical displacement considered in the measurement involves the rotation of the foot around the articulation of the ankle.

The testing apparatus includes the following main parts (see nomenclature in Figure 1):

1. Load cell (Interface 1500ASK-300) capturing the evolution of the reaction force as vibration starts. The load cell data acquisition frequency of 1 kHz granted a satisfactory sampling of experimental data. The load capacity of 1500 N is adequate for the typical force values to be measured in the experiments.
2. The impact on the concentrated mass M_w causes the vertical movement of the lower leg as a 1-degree-of-freedom system. It should be noted that the total oscillating mass M is actually equal to the

sum of M_w and the 1-degree-of-freedom equivalent mass of the lower limb.

3. and 4. Elements to accommodate the position of the person currently tested. Both the horizontal and vertical positions can be accommodated in several different locations, which are properly numbered. This allows the chair to be maintained in the same position, for the same person, if the test needs to be repeated. For any morphology of the subject, the three right angles indicated in Figure 1 must be granted in order to ensure the repeatability of measurements. To this end, the person is asked to maintain the back in contact with the backseat described in point 5.
5. The presence of the vertical backseat ensures, additionally to the former function, that the pressure on the load cell exercised by the foot be constant during measurements. The tested person must keep the back and the shoulders in contact with the backseat in order not to induce pressure variations that might be originated even by very simple movements of the subject's body during the test. Since the type of movement expected in the experiment involves the rotation of the thigh around the hip articulation in the plane of Figure 1, part of the thigh comes in contact with the seat (of 31 cm depth) as movements develop. However, this did not significantly interfere with the above-mentioned rotation of the thigh because the displacement values observed at the knee level were of the order of millimetres, involving rotations of the thigh of an order of milliradians ($\approx 0.1^\circ$). This small angle, together with the size of the seat (only a very short part of the thigh is in contact with the seat, see Figure 2), makes the upper leg to behave freely during the vibration. Furthermore, the thigh-seat contact zone recedes when the leg must hold the equilibrium position just before impact.



Figure 2. Global view of the experimental apparatus based on the measurement of lower leg vertical displacements.

6. The simply supported beam allows the loading system to be easily adapted to the anthropometrical features of the subject currently tested.
7. The supporting frame included a triangular structure in order to be enough rigid in the plane of Figure 1 thus not altering the free vibration behaviour of the system.

Figure 2 shows the testing apparatus and a person ready for the test. It can be seen that the arms of the subject were held in neutral position in order to avoid any interference with the measurement. This set-up can be utilized to test indifferently both legs (right and left)

without introducing any variation either in the position or in the interpretation of experimental data.

When an impulse is applied to the concentrated mass M_w , the total mass M (i.e. the 1-degree-of-freedom equivalent mass of the lower limb) starts to oscillate vertically as it is indicated in Figure 1. Figure 3(a) shows an arbitrary intermediate position for this movement. While distances L (length of the lower leg), R (forefoot distance from the articulation of the ankle) and r (rearfoot distance from the articulation of the ankle) remain constant during the vibration process, the length associated with the TS changes.

In this study, the TS complex was schematized according to the classical Hill's model¹⁵ by means of a spring of stiffness k and a damper of constant c . It is important to remark that the parallel elastic component (PEC) present in Hill's model has not been considered in this study (following Fukushima¹² and the references therein) as is not likely that the PEC significantly contributes to the induced oscillation movement. Since for the position represented in Figure 1 (i.e. 90° at the knee level) the gastrocnemius muscle does not work, the apparent values of stiffness k and damping c of the TS complex are relative to the soleus muscle and the Achilles tendon. For the clarity of representation, the equivalent TS spring-damper system sketched in the figure is inclined by a certain angle with respect to the direction corresponding to the lower leg. However, in the derivation of theoretical model, the TS was always considered parallel to the lower leg. The configurations shown in Figure 3 are referred to a fixed point corresponding to the contact

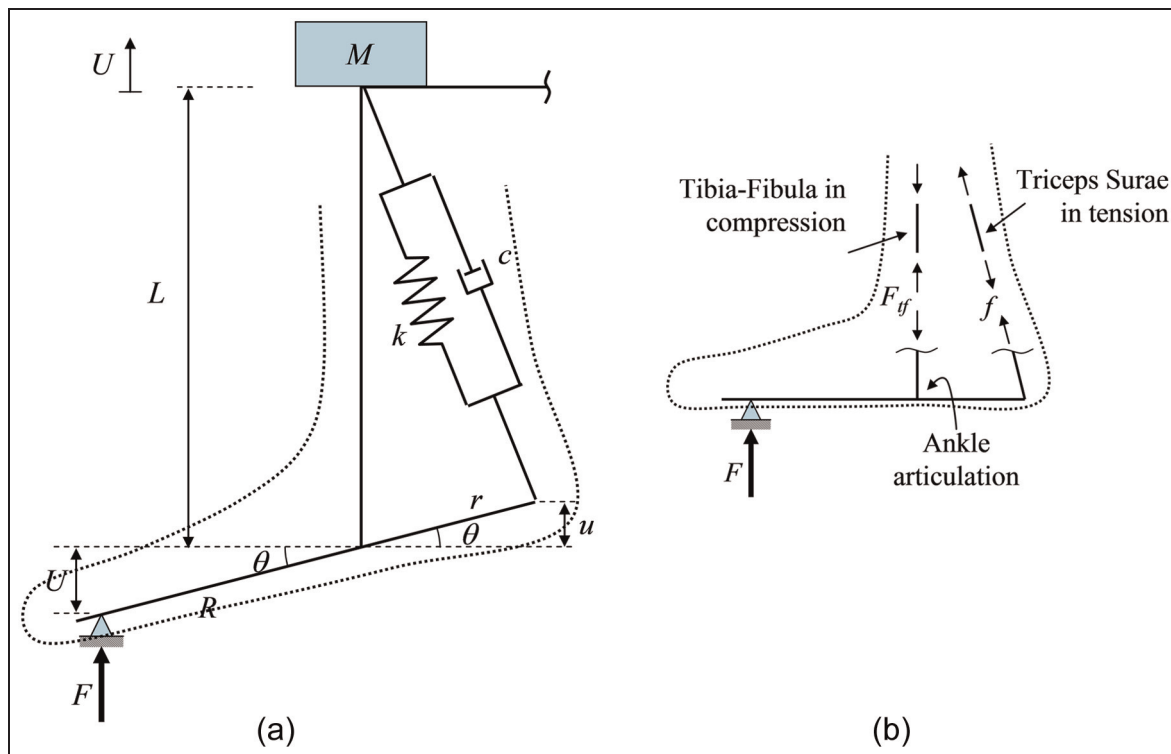


Figure 3. Experimental set-up based on the measurement of the vertical displacement of the lower leg: (a) simplified scheme of an arbitrary position taken in the vibration process and (b) forces involved in the equilibrium around the ankle.

region between the subject's foot and the load cell measuring the reaction force F .

The mass represented in Figure 3 is the total mass M involved in the movement, which is the sum of the concentrated mass M_w and the 1-degree-of-freedom equivalent mass representing in the model the distributed mass of the lower limb. Thus, M will represent the total 1-degree-of-freedom equivalent mass involved in the movement.

The displacements U and u indicated in Figure 3(a) are related to each other as follows

$$U = \frac{R}{r}u \quad (1)$$

The forces involved in the equilibrium around the ankle articulation are indicated in Figure 3(b): The force F_{tf} keeps the tibia–fibula set in compression while the force f keeps the TS complex in tension. From the condition of dynamic equilibrium of the forces schematized in Figure 3(b) with respect to the ankle articulation, it follows

$$(I + m_f r_G^2) \frac{d^2\theta}{dt^2} = FR \cos \theta - fr \cos \theta \quad (2)$$

where θ is the angle (Figure 3(a)) defining the instantaneous position of the foot, I is the momentum of inertia of the foot with respect to its centre of gravity, m_f is the mass of the foot involved in the movement and r_G is the distance between the centre of gravity of the foot and the centre of rotation. Note that the force corresponding to the weight of the leg and concentrated mass is aligned with the movement, its moment with respect to the axis of rotation being negligible in absolute terms.

The values of parameters in the left-hand side (LHS) of equation (2) were estimated from the previous studies^{16,17} Since these summands of the LHS of equation (2) are, in relative terms, much smaller than their counterpart for the right-hand side (RHS), equation (2) reduces to

$$FR = fr \quad (3)$$

The above equation allows the value of the force f passing through the line of action of the TS complex to be obtained once the value of the reaction force F is measured by the load cell, and the distances R and r are precisely determined for the tested foot.

The system in Figure 3(a) includes two coupled degrees of freedom: the rotation around the ankle articulation and the vertical displacement of the vibrating mass. Since the tibia–fibula set was assumed to be infinitely rigid,^{18,19} the vertical displacement of the mass M coincided with the vertical displacement of the ankle rotation point. The equivalent dynamic system hence corresponds to the 1-degree-of-freedom system schematized in Figure 4(a) where K and C are the apparent stiffness and the damping coefficient, respectively.

By taking as reference the configuration of the system including the external weight, the dynamic

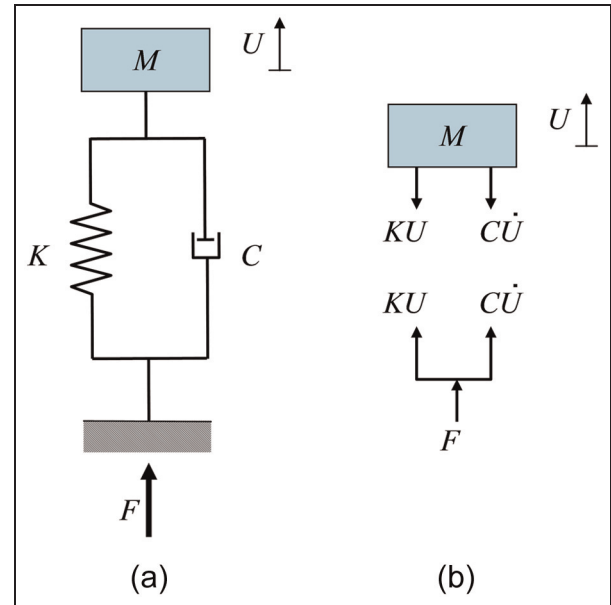


Figure 4. (a) Equivalent dynamic system including 1 degree of freedom and (b) force diagram.

equilibrium condition for the total mass M , after the impact, can be expressed as follows

$$M\ddot{U} = -KU - C\dot{U} \quad (4)$$

By disaggregating the system (see the scheme of forces in Figure 4(b)), it can be written as follows

$$F = -KU - C\dot{U} (= M\ddot{U}) \quad (5)$$

Should the reference configuration correspond to the instant preceding the application of the weight, a term ‘ $-M_s g$ ’ should be added in the RHS of equation (4). M_s represents the total static mass of the vibrating system (i.e. the mass that corresponds to the system that is vibrating, before to start the vibration). Note that this mass M_s does not have to exactly coincide with the total dynamic mass M involved in the movement. The reason is that while the part M_w of M is a concentrated mass, the remaining mass of M is a distributed mass, that of the lower limb. In a system of concentrated parameters, a unique mass, representing infinite points able to have different accelerations, is involved in the equation of motion with a unique value of acceleration. Thus, both masses, static and dynamic, correspond to different concepts. They would coincide if the acceleration was the same in all points of the actual distributed parameters system.

The general solution of the differential equation (4) written for an underdamped system is given as follows

$$U(t) = e^{-\xi\omega t} (A \sin \omega_D t + B \cos \omega_D t) \quad (6)$$

where the constants A and B are determined from the boundary conditions of the problem.

The damping factor ξ is defined as follows

$$\xi = \frac{C}{C_c} = \frac{C}{2M\omega} \quad (7)$$

where C is the damping of the system, C_c is the critical damping of the system, M is the total mass involved in the movement and ω is the natural frequency of the vibrating system.

The frequency of vibration ω_D of the damped system is given as follows

$$\omega_D = \omega\sqrt{1 - \xi^2} \quad (8)$$

By defining the parameter γ as

$$\gamma = \xi\omega = \frac{C}{2M} \quad (9)$$

it is possible to express the vibration frequency ω_D of the damped system as follows

$$\omega_D^2 = \omega^2 - \gamma^2 \quad (10)$$

The general expression of displacement (equation (6)) can be substituted in the equation of dynamic equilibrium (equation (5)). It is thus possible to express the total force F acting on the mass M as follows

$$F = (M\ddot{U}) = e^{-\gamma t}(A_F \sin \omega_D t + B_F \cos \omega_D t) \quad (11)$$

where A_F and B_F can be expressed in terms of M , A , B , γ and ω_D as $A_F = M(2B\gamma\omega_D + A(\gamma^2 - \omega_D^2))$ and $B_F = M(-2A\gamma\omega_D + B(\gamma^2 - \omega_D^2))$.

Since the load cell can sense the force (equation (11)) plus the action of gravity, the total force F_m measured in the experiments is given as follows

$$F_m = F + M_s g = e^{-\gamma t}(A_F \sin \omega_D t + B_F \cos \omega_D t) + M_s g \quad (12)$$

Because of the presence of weight, the sign of F_m is always negative (i.e. F_m is compressive) while the sign of force F depends on the equilibrium position.

Note that the variable γ involves (by means of equation (9)) the dynamic mass M participating in the movement. The static mass M_s could in principle be determined using the load cell, either before the impact or during the steady-state period after the attenuation of the signal. Then, the parameters γ , ω_D , A_F and B_F could be determined.

Due to the fact that in the two steady-state periods there are always small oscillations and that both values may be slightly different due to small movements of the subject, the accurate identification of M_s is not a straightforward task. Additionally, due to the dominant role of the concentrated mass in the total dynamic mass, it is expected that the behaviour of the system is correctly represented assuming ($M_s \approx M$), a typical assumption followed in the previous studies.¹²⁻¹⁴

With this hypothesis, equation (12) includes the unknown parameters γ , ω_D , A_F , B_F and M ($M \approx M_s$) that must be determined with the least-square fitting

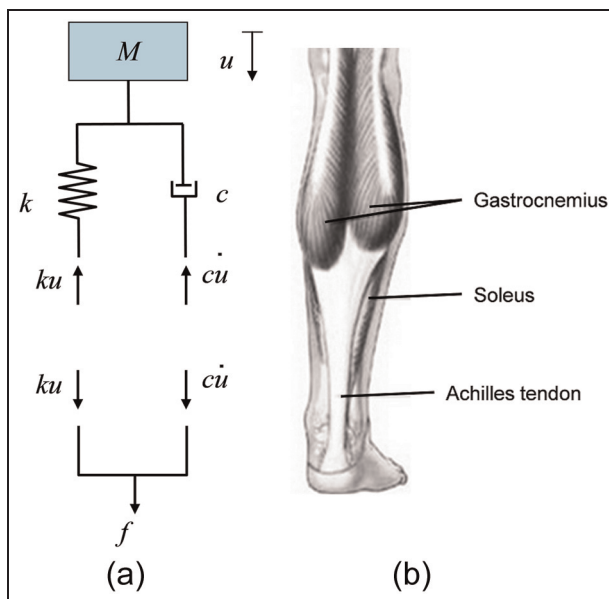


Figure 5. Force diagram for the equivalent dynamic system of TS muscle–tendon complex. (a) Schematic representation, (b) TS components.

procedure described in the ‘Forefoot and rearfoot distances measurement’ section.

Once these unknown parameters are determined, the values of apparent stiffness K and damping C of the whole system can be determined as follows

$$K = M(\omega_D^2 + \gamma^2) \quad (13)$$

$$C = 2\gamma M \quad (14)$$

The parameters K and C can be related to the apparent stiffness k and damping c of the TS complex. For this purpose, the condition of dynamic equilibrium can also be written for the TS by referring to the load diagram shown in Figure 5(a). An illustration of the TS and its constituents (soleus, gastrocnemius and Achilles tendon), to which Figure 5(a) represents, is shown in Figure 5(b)

$$f = -ku - c\dot{u} \quad (15)$$

By substituting equations (1) and (3) into equation (5) and rearranging the expression, it follows

$$f = -\left(\frac{R}{r}\right)^2 Ku - \left(\frac{R}{r}\right)^2 C\dot{u} \quad (16)$$

Since equations (15) and (16) are equivalent, all terms contained in these expressions must coincide. The following conditions can hence be obtained

$$k = \left(\frac{R}{r}\right)^2 K, \quad c = \left(\frac{R}{r}\right)^2 C \quad (17)$$

A very important issue entailed by the above described model is the precise determination of the values of r and R for the tested person. This aspect is discussed in detail in the ‘Forefoot and rearfoot distances measurement’ section and in the study by Paris-García.²⁰

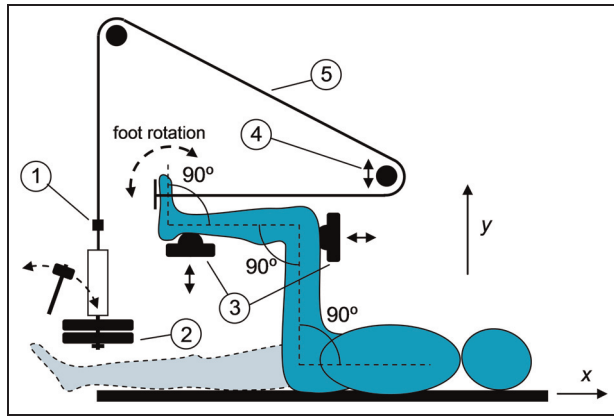


Figure 6. Schematic diagram of the experimental set-up for determining TS visco-elastic properties based on the rotation of the foot around the ankle articulation.

TS identification procedure based on the rotation of the foot around the ankle articulation

The experimental apparatus was designed following the measurement approach described in the study by Babic and Lenarcic.¹³ The basic idea is to generate a configuration of the human body by allowing only the rotation of the foot around the articulation of the ankle. The overview schematic of the testing apparatus is shown in Figure 6. The configuration of the equipment may be easily arranged so as to have the leg in complete extension thus putting the gastrocnemius in free vibration. However, since the main objective of this study was to critically compare previous studies,^{12,13} only the configuration shown in Figure 6 was considered.

The testing apparatus includes the following main parts (see nomenclature in Figure 6):

1. The same load cell used in the previous experiments (Interface 1500ASK-300) was utilized to monitor the evolution of the force transferred by the wire during vibration.
2. The impact on the concentrated mass M_w causes the rotation of the foot around the articulation of the ankle as a 1-degree-of-freedom system. It should be noted that the total oscillating mass M , independently of the foot, is actually equal to the sum of M_w and the mass of the whole system associated with the movement of the wire. As in the previous case, since it may not be an easy task to identify the actual value of M , the total oscillating mass M was included as an additional parameter in the fitting process. The total mass M was located in the same position as M_w (see Figure 8) because its position does not affect the equation of movement. For this load case, the mass m_f of the foot was considered separately. The movement was produced by applying an impulsive load to the mass M_w .
3. and 4. Elements to accommodate the position of the person currently tested. For any morphology

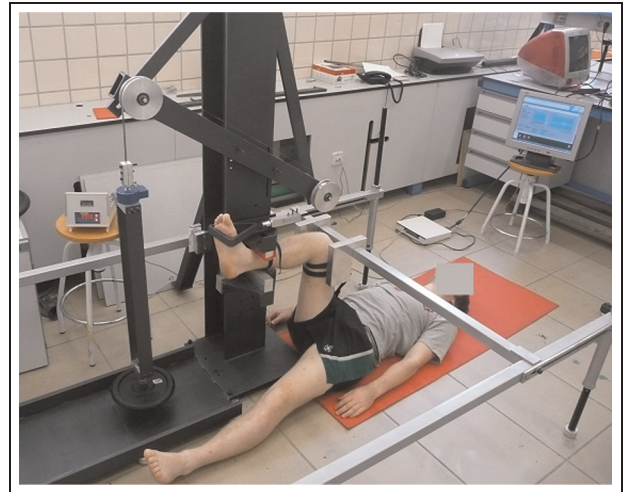


Figure 7. Global view of the experimental apparatus based on the measurement of the rotation of the foot around the ankle articulation.

of the subject, the three right angles indicated in Figure 6 must be granted and the rotation of the foot around the ankle articulation must be the only movement allowed. This ensured the validity of measurements.

5. The system transferring the load from the weight to the foot was composed of a steel wire and two pulleys. The wire was very stiff with respect to tensile forces and flexible enough with respect to bending in order to easily adapt to the local shape of pulley channel. After several trials, the cross section of the wire was selected as a thin rectangular steel lamina of width 17 mm and thickness 0.5 mm. The position of the pulley placed at the level of the foot (i.e. the pulley closest to the foot in the direction of transferred load) was tuneable in height thus allowing the final part of the wire to be held horizontal near the subject's foot.

The disposition presented in the 'TS identification procedure based on the vertical displacement of the lower leg' section can be used in a natural form for both legs. However, the disposition associated with present procedure requires either to conceive a very unique complicated device to test both legs or to design a simpler one but applicable only to one leg. The second option was selected, and a testing apparatus for the right leg (Figure 7) was designed and built. To try to use the apparatus shown in Figure 7 and to test the left leg would imply the subject to take a forced posture where the right leg would be placed unnaturally in the right side of the structure, which can significantly affect the measurements.

In order to derive the theoretical model describing the dynamic behaviour of the system under free vibration, the reference scheme of Figure 8 was considered. The distance R between the origin of the reference system and the line of action of the equivalent force acting

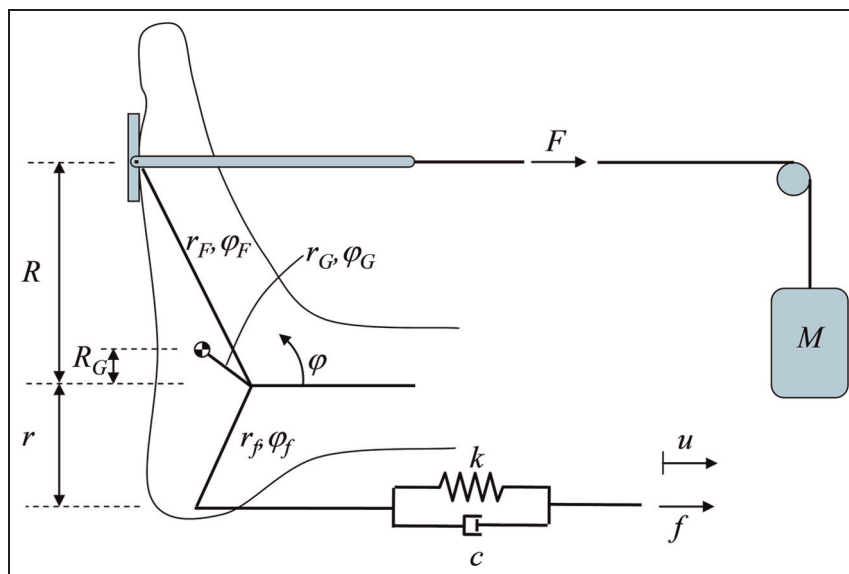


Figure 8. Experimental set-up based on the measurement of the rotation of the foot around the ankle articulation: simplified scheme of the foot functioning during the free vibration.

on the total mass M , the distance R_G between the origin of the reference system and the centre of gravity of the foot, and the distance r between the origin of the reference system and action line of the Achilles tendon can be expressed as follows

$$\begin{aligned} R &= |r_F \sin \varphi_F| \\ R_G &= |r_G \sin \varphi_G| \\ r &= |r_f \sin \varphi_f| \end{aligned} \quad (18)$$

Under the hypothesis of infinite stiffness in tension of the wire, the condition of momentum equilibrium written with respect to the equilibrium position (i.e. after applying the mass M_w) can be stated as follows

$$(I + m_f R_G^2 + MR^2)\ddot{\varphi} = fr \quad (19)$$

where I has been previously defined, φ is the angle that defines the position of the foot during the vibration movement and f is the reaction force developed in the MTC.

The reaction force f developed in the MTC is the sum of the contribution of a spring of stiffness k and a damper of damping coefficient c . It can be written as follows

$$f = -ku - c\dot{u} = -k\varphi r - c\dot{\varphi} r \quad (20)$$

where the relationship $u = \varphi r$ between φ and u is derived from Figure 8.

By substituting the last equality of equation (20) in the RHS of equation (19) and rearranging the terms, the dynamic equilibrium equation describing the movement of the system can be obtained as follows

$$(I + m_f R_G^2 + MR^2)\ddot{\varphi} + cr^2\dot{\varphi} + kr^2\varphi = 0 \quad (21)$$

Similar to the previous loading condition, the terms relative to the inertia of the foot are negligible with respect to MR^2 . Therefore, equation (21) reduces to

$$MR^2\ddot{\varphi} + cr^2\dot{\varphi} + kr^2\varphi = 0 \quad (22)$$

The simplifying assumption leading to equation (22) makes it unnecessary to measure the position of the centre of gravity of the foot.

The general solution of the differential equation (22) is given as follows

$$\varphi(t) = e^{-\gamma t}(A \sin \omega_D t + B \cos \omega_D t) \quad (23)$$

hence analogous to the general displacement solution (equation (6)) derived in the 'TS identification procedure based on the vertical displacement of the lower leg' section.

The values of γ and ω_D are respectively defined as follows

$$\gamma = \frac{cr^2}{2MR^2} \quad (24a)$$

$$\omega_D^2 = \frac{kr^2}{MR^2} - \gamma^2 \quad (24b)$$

By combining equations (24a) and (24b), the viscoelastic parameters k and c of the TS complex can be obtained as follows

$$k = \frac{MR^2}{r^2}(\omega_D^2 + \gamma^2) \quad (25a)$$

$$c = \frac{2MR^2}{r^2}\gamma \quad (25b)$$

In order to determine the values of k and c , one has to determine γ and ω_D first by measuring the force developed in the wire as the impulsive load is applied.

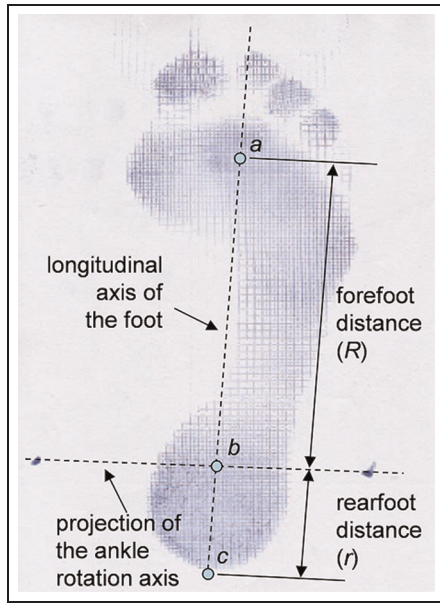


Figure 9. Forefoot and rearfoot distance measurements by means of a pedigraphy.

This force, which is registered by the load cell, can be expressed as follows

$$F_m(t) = M(g + \ddot{\varphi}R) \quad (26)$$

The assumption that $M_s \approx M$ reasoned in the ‘TS identification procedure based on the vertical displacement of the lower leg’ section will also be employed in this section, as done in equation (26) with reference to the term $M_s g$.

If the displacement solution of equation (23) is derived twice with respect to time, the following expression is obtained

$$\ddot{\varphi}(t) = e^{-\gamma t}(A_a \sin \omega_D t + B_a \cos \omega_D t) \quad (27)$$

where A_a and B_a can be expressed in terms of A , B , γ and ω_D as $A_F = (2B\gamma\omega_D + A(\gamma^2 - \omega_D^2))$ and $B_F = (-2A\gamma\omega_D + B(\gamma^2 - \omega_D^2))$.

By substituting equation (27) in the RHS of equation (26), the final expression of the force to be measured is given as follows

$$F_m = F(t) = e^{-\gamma t}(A_F \sin \omega_D t + B_F \cos \omega_D t) + Mg \quad (28)$$

where A_F and B_F can be expressed in terms of M , R , A , B , γ and ω_D as $A_F = MR(2B\gamma\omega_D + A(\gamma^2 - \omega_D^2))$ and $B_F = MR(-2A\gamma\omega_D + B(\gamma^2 - \omega_D^2))$

Equation (28) includes the unknown parameters γ , ω_D , A_F , B_F and M that must be determined with the least-square fitting procedure described in the ‘Processing of experimental data and extraction of TS visco-elastic parameters’ section. Equation (25) must hence be used to evaluate MTC visco-elastic parameters k and c .

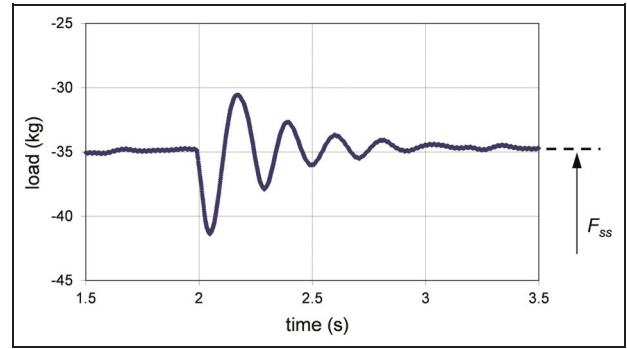


Figure 10. Typical force–time diagram registered by the load cell.

Similar to the loading case previously considered, the values determined for parameters k and c may be strongly sensitive to the ratio R/r . Therefore, once forefoot and rearfoot distances R and r were determined for a subject, special cares must be taken in placing the foot always in the correct position (i.e. the second metatarsal head must be in contact with the transmission device). This position must be the same for both loading cases in order to have a homogeneous basis of comparison for the visco-elastic parameters extracted from the two in vivo procedures considered in this study.

Forefoot and rearfoot distances measurement

A non-invasive procedure based on pedigraphies, to obtain the lever arms of the forefoot (R) and rearfoot (r), has been developed. The procedure has two phases: the first is to obtain a footprint, by means of a pedigraphy, indicating on it a certain number of anatomical references. In a second phase, a procedure for locating the necessary three points of reference is followed. The three points, indicated as a , b and c in Figure 9, are placed along the longitudinal axis of the foot and their location allows us to obtain the desired lever arms.

Point a is located at the position of the resultant of the distribution of pressure in the forefoot. Point b represents the intersection point between the projection of the ankle rotation axis and the longitudinal axis of the foot. Finally, c represents the projection of the Achilles tendon axis on the footprint plane. In this way, the positions a , b and c determine the distances R and r , as indicated in Figure 9. A more detailed description of the procedure can be found in the study by París-García.²⁰

Processing of experimental data and extraction of TS visco-elastic parameters

Reaction force values were recorded by the load cell at regular time intervals. A typical force–time plot is shown in Figure 10 where the steady-state value finally reached by F is denoted as F_{ss} . The plot in Figure 10 is

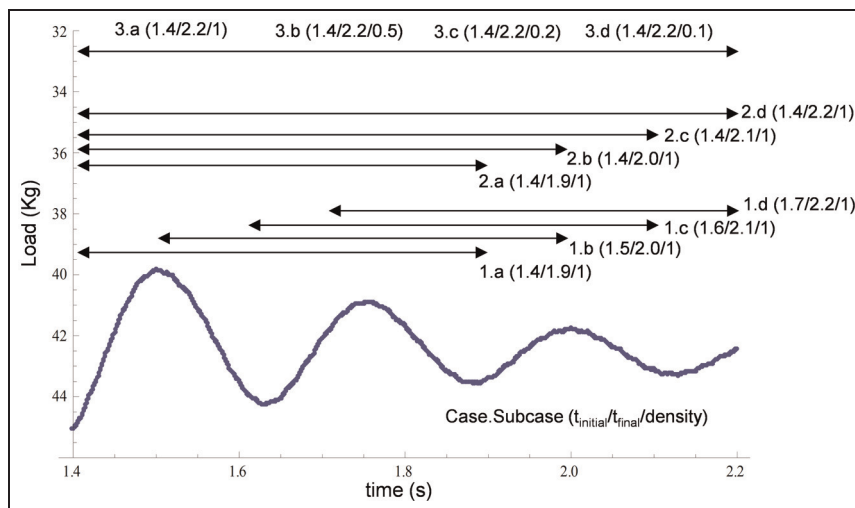


Figure 11. Sensitivity parameters analysed in order to optimize the fitting process.

relative to the measurement protocol described in the ‘TS identification procedure based on the vertical displacement of the lower leg’ section and was obtained for a nominal weight of 25 kg. The nominal value of applied load was recovered after the vibration period originated by the impulsive load. The steady-state force value indicated in the figure is about 35 kg, that is, 10 kg higher than the nominal weight of 25 kg. This is because of the presence of the weight of the lower leg involved in the vibration process. Note that all values of the load cell are negative due to the fact that the load cell is in compression.

The equivalent force measured by the load cell for the two experimental procedures described in the ‘TS identification procedure based on the vertical displacement of the lower leg’ and the ‘TS identification procedure based on the rotation of the foot around the ankle articulation’ sections always has the same expression (i.e. equations (12) and (28) for the first and the second loading cases, respectively). The instantaneous force value always depends on the following five parameters: the damping coefficient γ , the vibration frequency of the damped system ω_D , the total mass M involved in the movement (after the identification of M_s and M), and the coefficients A_F and B_F .

In order to determine the unknown parameters listed above, one can minimize the error functional Ω corresponding to the difference between the values of force measured by the cell and their counterpart predicted by numerical models as follows

$$\Omega = \sum_{i=1}^n [F_{\text{exp}}(t_{\text{exp}}) - F(\gamma, \omega_D, A_F, B_F, M)]^2 \quad (29)$$

where n is the number of control points (i.e. experimentally recorded data) to be included in the fitting procedure; F_{exp} is the force value experimentally measured at the sampling time t_{exp} ; and F is the force value predicted

by the theoretical model based on the assumption of a 1-degree-of-freedom system.

The error functional Ω was minimized in the least-square sense. In general, the fitting procedure should always converge to the global minimum. However, there are some aspects to be considered. In the first place, the probability of reaching the global optimum may depend significantly on the ranges of variation chosen for the five unknown parameters involved in the fitting procedure. Furthermore, optimization behaviour may be sensitive to the initial values set for the fitting parameters that should always be chosen in view of their physical meaning or on the basis of previous experience acquired for similar problems. In particular, very accurate estimations of the initial values of M , γ and ω_D can be obtained from the experimental data, the first as the value before (and after) the perturbation, the second as the decay of consecutive peaks of the oscillating signal and the third as measuring the time interval between consecutive peaks of the signal. Other critical aspects are how to select the time interval in which experimental data must be recorded either in terms of the size and position of the interval or the number of control points where the error functional Ω must be evaluated.

A sensitivity study was carried out in this research in order to optimize the performance of the fitting procedure. All cases considered in the parametric analysis are summarized by Figure 11. The experimental curve taken as an example in Figure 11 corresponds to the first procedure (‘TS identification procedure based on the vertical displacement of the lower leg’ section), reason by which the reaction force (data in the vertical axis) presents negative values, the load cell being always in compression. The following general nomenclature was adopted: case.subcase (t_{initial} , t_{final} , density). Density = 1 means that all data points were used to build the error functional Ω , while density = 0.1 means that only 1 data point of every 10 data points was used.

Table 1. Values of k and c obtained in the parametric study.

	a	b	c	d	Mean	SD	CV (%)
Values of k (kN/m)							
Case 1	187.34	189.84	195.62	195.59	192.10	4.17	2.17
Case 2	187.34	187.73	189.04	188.75	187.47	1.96	1.05
Case 3	188.75	188.74	188.72	188.68	188.72	0.03	0.02
Values of c (N s/m)							
Case 1	1216.3	1290.7	1376.3	1657.8	1385.3	193.09	13.94
Case 2	1216.3	1288.2	1387.4	1290.4	1295.5	70.23	5.42
Case 3	1290.4	1289.5	1286.5	1281.9	1287.1	3.79	0.29

SD: standard deviation; CV: coefficient of variation.

Case 1. For fixed sizes (i.e. between 1.4 and 1.7 s) of the data time interval, different time origins were chosen for the experimental force–time plots. Subcase ‘a’ corresponds to $t_{\text{initial}} = 1.4$ s, subcase ‘b’ corresponds to $t_{\text{initial}} = 1.5$ s, subcase ‘c’ corresponds to $t_{\text{initial}} = 1.6$ s and subcase ‘d’ corresponds to $t_{\text{initial}} = 1.7$ s.

Case 2. For a fixed time origin (i.e. 1.4 s), different sizes of the time interval were considered. Subcase ‘a’ corresponds to a time interval of 0.5 s, subcase ‘b’ corresponds to a time interval of 0.6 s, subcase ‘c’ corresponds to a time interval of 0.7 s and subcase ‘d’ corresponds to a time interval of 0.8 s.

Case 3. For a fixed origin (i.e. 1.4 s) and size (i.e. 2.2 s) of the time interval, different densities of the experimental data points were chosen in order to build the error functional Ω . Subcase ‘a’ corresponds to density = 1, subcase ‘b’ corresponds to density = 0.5, subcase ‘c’ corresponds to density = 0.2 and subcase ‘d’ corresponds to density = 0.1.

The results of sensitivity analysis obtained for the stiffness coefficient k and the damping coefficient c are summarized in Table 1. Remarkably, the result of fitting process does not significantly depend on the size and the position of time data interval as well as it is independent of sampling. The coefficient of variation (CV) defined as the ratio between the standard deviation (SD) and the average value was always lower than 3%. The same sensitivity study was carried out for the experimental data obtained from the second procedure. Analogous qualitative and quantitative results were obtained, but they have not been included here for the sake of brevity.

The results found showing the insensitivity of the procedure to size and position of the interval under study, give confidence on the robustness of the procedure itself. Moreover, the results suggested a criterion for choosing the data interval where to carry out the fitting process. The data interval was set to be the largest in size and with the maximum density by including all possible data points. In general, the largest size of the data time interval is determined by two transient effects

in the beginning and at the end of the vibration period. The experimental data may initially appear irregular just after the instant at which impact occurs because of the transient effect of the impact itself (this is consistent with other study reported in the literature: see, for example, Figure 2 of Fukushima et al.¹²). Data relative to the final part of the vibration process when the oscillation is almost completely damped also should be avoided as the signal-to-noise ratio may get close to 1. By cutting properly the initial and final parts of the data time interval, it is possible not to introduce numerical disturbances in the fitting process.

Once the values of the five unknown parameters were determined by minimizing the error functional Ω (equation (29)), the values of stiffness K and damping C of the equivalent vibrating system were calculated with equations (13) and (14) for the first load case. The reaction force f developed in the TS was calculated with equation (16). Equation (17) finally provided the apparent values of stiffness k and damping c of the TS.

For the second loading case, equation (16) was again used to evaluate the reaction force f developed in the TS. Finally, equation (25) allowed visco-elastic parameters k and c to be determined.

Results and discussion

The apparent values of stiffness k and damping c were determined for a population including seven male and three female subjects. Each subject was submitted to both loading conditions in order to have a homogeneous basis of comparison between the two measurement protocols. The right leg of each subject was tested as this was the case for which both equipments developed were fully usable. The characteristics of the population in terms of sex, age, height, weight and R/r ratio are summarized in Table 2. For comparison purposes, representative values of populations of previous studies^{12,13} have also been included in Table 2.

As can be seen, the average age of the populations of the three studies is quite similar as well as the size of the population (6 in Fukushima et al.,¹² 10 in Babic and Lenarcic¹³ and 10 in this study). However, while height and weight are quite similar in what respect to this study and the study by Babic and Lenarcic,¹³ they both

Table 2. Characteristics (sex, age, height, weight and R/r ratio) of the tested subjects.

Subject	Sex	Age (years)	Height (m)	Weight (kg)	R/r
1	Male	34	1.88	95	2.65
2	Male	21	1.76	75	2.71
3	Male	32	1.94	98	2.93
4	Male	21	1.75	77	2.59
5	Male	37	1.78	84	2.17
6	Male	24	1.75	80	3.12
7	Male	29	1.74	70	2.97
8	Female	31	1.73	54	2.94
9	Female	31	1.60	56	2.64
10	Female	32	1.72	60	2.61
Reference	Population	Mean/SD	Mean/SD	Mean/SD	
This study	7 males; 3 females	29/5.5	1.77/0.09	74.9/15.2	
Fukashiro et al. ¹²	4 males; 2 females	25/1.9	1.63/0.06	60.2/5.7	
Babic and Lenaric ¹³	10 males	26/4.0	1.80/0.06	77.1/7.2	

SD: standard deviation.

are significantly higher than those corresponding to the population of the study by Fukashiro et al.¹²

For each load level, experimental tests were replicated four times to check the level of repeatability of measurements. For this purpose, tests were performed sequentially without altering the general configuration of the testing apparatus and taking a proper time interval lasting several seconds between each replication. In particular, the foot position was unaltered (no repositioning) during these four tests. In this way, although there is a device to reproduce the position of the foot in the load cell in all tests, uncertainties in the values of R/r are completely avoided.

Figures 12 and 13 show the results obtained in the case of a 30-kg applied weight for the first loading case described by the vertical translation of the lower leg and the second loading case described by the rotation of the foot around the ankle articulation, respectively. The plots present the evolution of the reaction force (F) sensed by the load cell during the tests. The experimental data appear superimposed on the corresponding theoretical values predicted by the 1-degree-of-freedom models to which the parameter values obtained from the fitting procedure described in the 'Forefoot and rearfoot distances measurement' section were given as input. Note that while in Figure 12 the value of the signal (F) oscillates around a value between 41 and 42 kg, in Figure 13 it oscillates around a value between 32 and 33 kg. In both figures, the applied weight is the same (30 kg), but in the first procedure (Figure 12), there is an additional oscillating mass of the lower part of the leg that produces an additional weight of around 11 kg, whereas in the second procedure (Figure 13), the additional weight involved in the oscillation is only around 2.5 kg. The figures are relative to subject 1. Since data trends obtained for the other subjects are very similar, they will not be reported in this article for the sake of brevity.

The results below each plot in Figures 12 and 13 include the steady-state value of the reaction force f_{ss} developed in the TS after the stabilization of the

vibration signal. This quantity was obtained from the steady-state force value F_{ss} measured by the load cell (see Figure 10) and using equation (3). The values of apparent stiffness k and viscosity c obtained via least-square fitting are also indicated in the figure. The maximum and minimum values, range of variation, average value, SD and the CV for f_{ss} , k and c are reported for both testing protocols. The time interval utilized in the fitting process for each test replication changed in function of the structure (i.e. shape, quality, etc.) of the signal. The experimental data were pre-processed to remove signal disturbances appearing in the beginning and at the end of the measurement period.

By analysing the force-time plots shown in Figures 12 and 13, the presence of a secondary frequency mixed with the fundamental vibration frequency can be observed. The secondary frequency depends on the natural oscillation of the equipment structure and should be at least 2.5 times higher than the MTC frequency in order not to perturb the measured TS frequency.²¹ The natural frequency of the testing apparatus was measured by performing vibration tests without human subjects. The apparatus was submitted to an impulse, and the corresponding vibration response was recorded by the load cell. Modifications aimed at increasing the stiffness of the testing apparatus allowed the natural frequency of the structure to be 90–100 rad/s, that is, more than 3 times higher than the MTC natural frequency (20–30 rad/s) registered for the tested subjects. Therefore, the secondary vibration frequency of the structure does not affect significantly the measurement of the MTC mechanical properties.

An excellent agreement between the experimental data recorded by the load cell and the numerical results derived from the fitting process can be observed from Figures 12 and 13. Therefore, the mechanical behaviour of the vibrating systems entailed by the two experimental set-ups was efficiently described by the 1-degree-of-freedom systems developed in the 'Determination of visco-elastic properties of the human TS MTC' section.

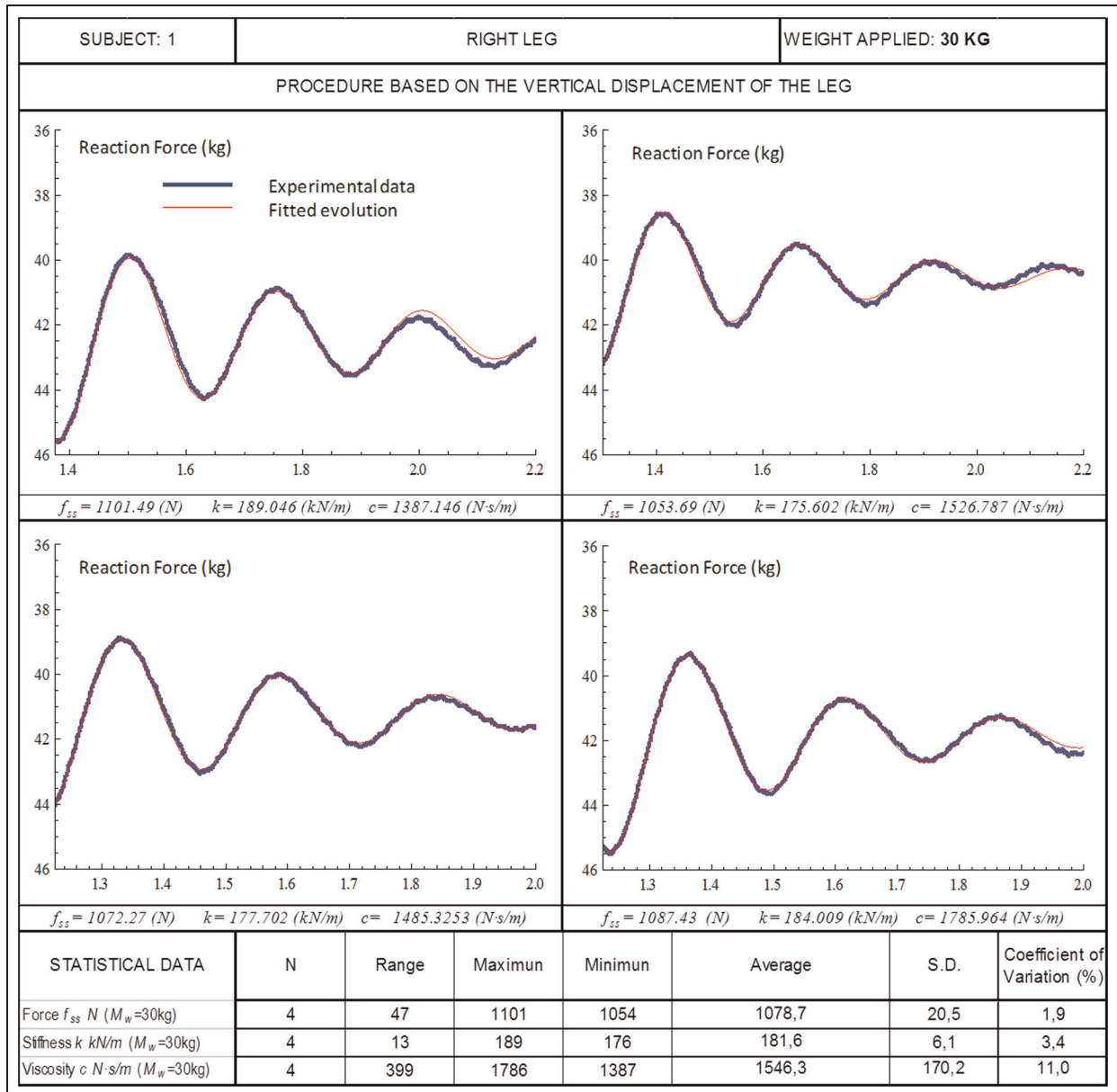


Figure 12. Reaction force F versus time results obtained for subject I for the loading case based on the measurement of the vertical displacement of the right leg.

The steady-state force f_{ss} developed in the MTC presents a statistical dispersion of about 2% in the case of the first loading case. Negligible dispersion occurs for the four test replications performed in the second load case. The statistical dispersion on f_{ss} can be explained by the fact that modifying the subject's position towards front or back implies variations in the reaction force that the foot generates on the load cell. The testing apparatus was properly adjusted to minimize this effect, which instead is not important for the second loading case as the subject's back lies on the floor.

In the case of the first testing apparatus, the 1.9% CV found for the reaction force f_{ss} developed in the TS entails a CV equal to 3.4% and 11% for apparent stiffness k and viscosity c , respectively. The higher dispersion

found for mechanical properties can be explained in view of the variations in vibration frequency observed for different replications. Furthermore, the MTC force f_{ss} is proportional to the stiffness which in turns depends on the square of vibration frequency.

For the second loading case, the CV for the f_{ss} force dropped to 0%, while the values of the CV found for the apparent stiffness and viscosity parameters are 5.6% and 19.9%, respectively.

The results obtained for the whole weight range (i.e. between 10 and 40 kg) considered in the experimental campaign carried out in this study is summarized in Tables 3 and 4, as an illustrative example, for subject 1. The tables list the reaction force f_{ss} , apparent stiffness k and viscosity c and the corresponding average values, SDs and CVs.

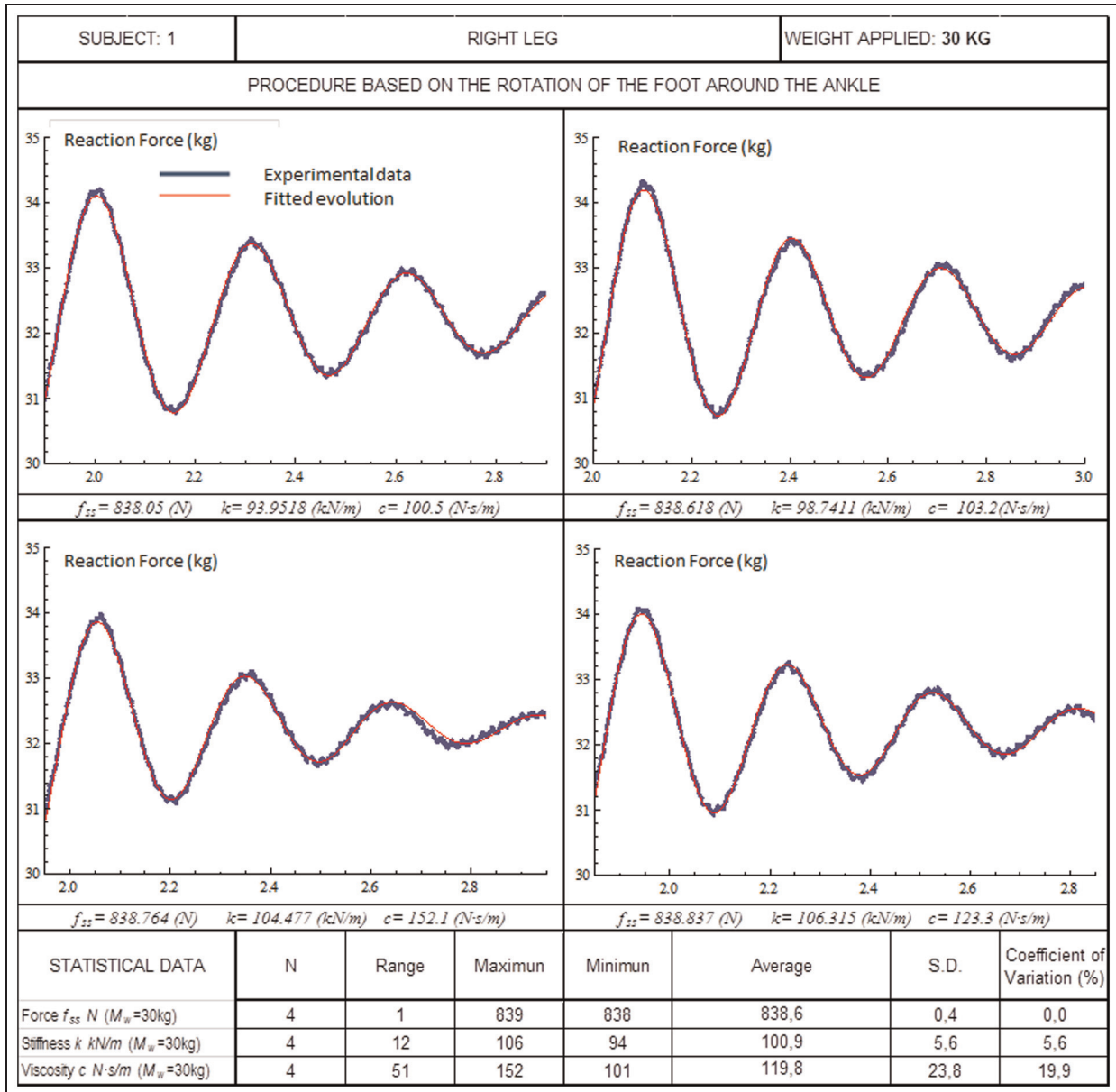


Figure 13. Reaction force F versus time results obtained for subject 1 in the loading case based on the measurement of the rotation of the foot around the ankle.

In order to better assess the relationships between mechanical properties k and c and the applied weight, average results obtained in the experimental tests are plotted in Figures 14 and 15, respectively, for apparent stiffness and viscosity (the figures include range bars for the minimum and maximum values). The apparent stiffness k increased with the applied load for all subjects. The same behaviour was seen for both loading cases and can be explained in view of the contribution given to the reaction force by the soleus muscle whose stiffness depends on the magnitude of applied load. The relationship between the viscosity c and the applied load is less clear than in the case of stiffness. In any case, to assume, as in many simplified models, that viscosity presents a constant value versus the applied load, seems a plausible assumption, in view of the results obtained.

It is clearly shown in Figures 14 and 15 that the TS mechanical properties are systematically different when measured using one or the other procedure. To make it even clearer, Figure 16 shows the value of the apparent stiffness (for 25 kg) for all subjects measured using both procedures. In particular, Figure 16(a) shows absolute stiffness values and Figure 16(b) shows the ratio of stiffness values measured by the two procedures (rotation of the foot/vertical displacement). From Figure 16(a), it is clear that stiffness values strongly depend on the subject. From Figure 16(b), it can be appreciated that the procedure based on the rotation of the foot, systematically yields lower values (approximately 50% in this study), and this fact shows a strong consistency as it is almost the same for the 10 tested subjects. With reference to viscosity values, the trend observed is similar, the procedure based on the vertical displacements

Table 3. Results obtained for the force developed in the TS complex by considering the vertical displacement of the lower leg (subject 1).

Values of f_{ss} , k and c		Test number				Average	SD	CV
		Test 1	Test 2	Test 3	Test 4			
10 kg	f_{ss}	560	563	582	610	579	22.7	3.9
	k	139	130	143	157	142	11	8
	c	1291	1430	1245	1444	1353	99.8	7.4
15 kg	f_{ss}	683	695	735	737	712	28	4
	k	137	153	159	167	154	13	8
	c	1468	1713	1442	1426	1512	135.1	8.9
20 kg	f_{ss}	797	813	827	844	820	20	2
	k	148	156	157	162	156	5	4
	c	1669	1639	1767	1750	1706	61.9	3.6
25 kg	f_{ss}	946	975	983	983	972	18	2
	k	166	170	184	166	172	8	5
	c	1668	1578	1466	1604	1579	84.6	5.4
30 kg	f_{ss}	1054	1072	1087	1101	1079	21	2
	k	189	176	178	184	182	6	3
	c	1387	1527	1485	1786	1546	170.2	11.0
35 kg	f_{ss}	1114	1124	1152	1169	1140	25	2
	k	178	184	185	196	186	8	4
	c	1735	1596	1391	1556	1570	141.8	9.0
40 kg	f_{ss}	1199	1230	1258	1305	1248	45	4
	k	168	188	200	189	186	13	7
	c	1673	1747	2284	1597	1825	311.7	17.1

SD: standard deviation; CV: coefficient of variation.

Table 4. Results obtained for the force developed in the TS complex by considering the rotation of the foot around the ankle articulation (subject 1).

Values of f_{ss} , k and c		Test number				Average	SD	CV
		Test 1	Test 2	Test 3	Test 4			
10 kg	f_{ss}	363	363	363	364	363	0.4	0.1
	k	55	59	55	55	56	1.7	3.0
	c	534	511	488	453	496	34.8	7.0
15 kg	f_{ss}	488	488	489	490	489	0.8	0.2
	k	69	64	71	71	69	3.4	5.0
	c	582	599	599	574	588	12.6	2.1
20 kg	f_{ss}	599	600	600	601	600	1.0	0.2
	k	77	82	85	80	81	3.6	4.4
	c	725	965	597	774	765	152.3	19.9
25 kg	f_{ss}	726	726	726	728	727	0.9	0.1
	k	92	92	91	93	92	0.9	1.0
	c	625	879	744	809	764	108.1	14.2
30 kg	f_{ss}	838	839	839	839	839	0.4	0.0
	k	94	99	104	106	101	5.6	5.6
	c	706	725	1069	866	841	167.4	19.9
35 kg	f_{ss}	963	964	964	966	964	1.3	0.1
	k	104	108	117	110	110	5.4	4.9
	c	970	1035	995	869	967	70.9	7.3
40 kg	f_{ss}	1080	1082	1083	1083	1082	1.2	0.1
	k	114	127	115	142	124	13.0	10.4
	c	1153	913	1024	1590	1170	296.7	25.4

SD: standard deviation; CV: coefficient of variation.

giving systematically higher values than the procedure based on the rotation of the foot.

Table 5 shows the results for the TS stiffness (k) obtained for all tested subjects, right leg, and 25 kg of applied weight, using the procedure described in the

‘TS identification procedure based on the vertical displacement of the lower leg’ and the ‘TS identification procedure based on the rotation of the foot around the ankle articulation’ sections. Table 6 show the corresponding results for TS viscosity (c) and for the 10

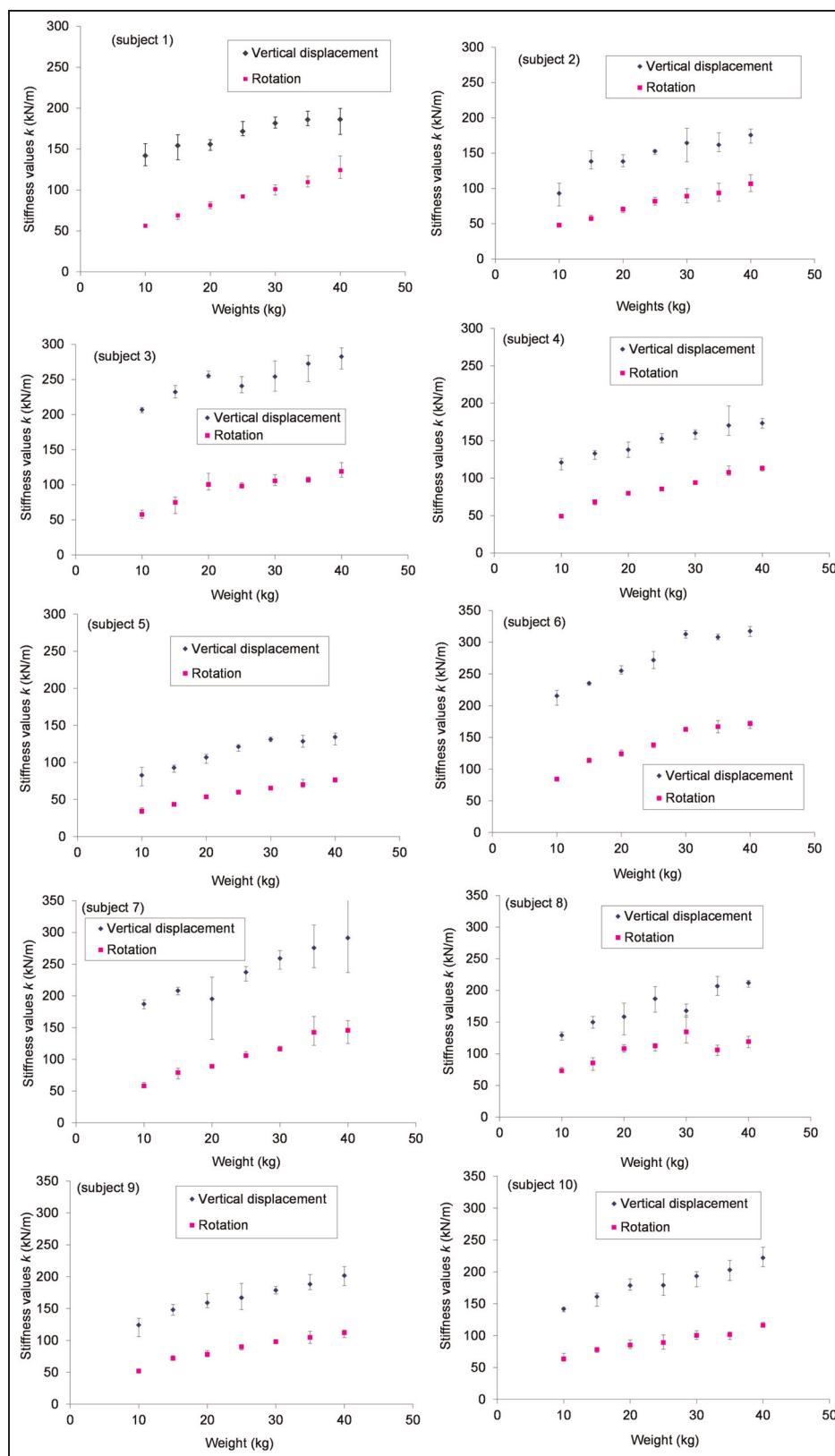


Figure 14. Variation of the apparent stiffness of TS complex with respect to the nominal applied load for the 2 measurement protocols and for the 10 tested subjects.

tested subjects, right leg and 25 kg. The results for stiffness in Table 5 (first procedure) indicates that for each subject, a reasonably low dispersion was found in the results. Nevertheless, the mean values differ

significantly from one subject to another (values varying from 121 kN/m in subject 5 to 272 kN/m in subject 6). The same trend is observed in Table 5 for the procedure based on the rotation of the foot around the ankle

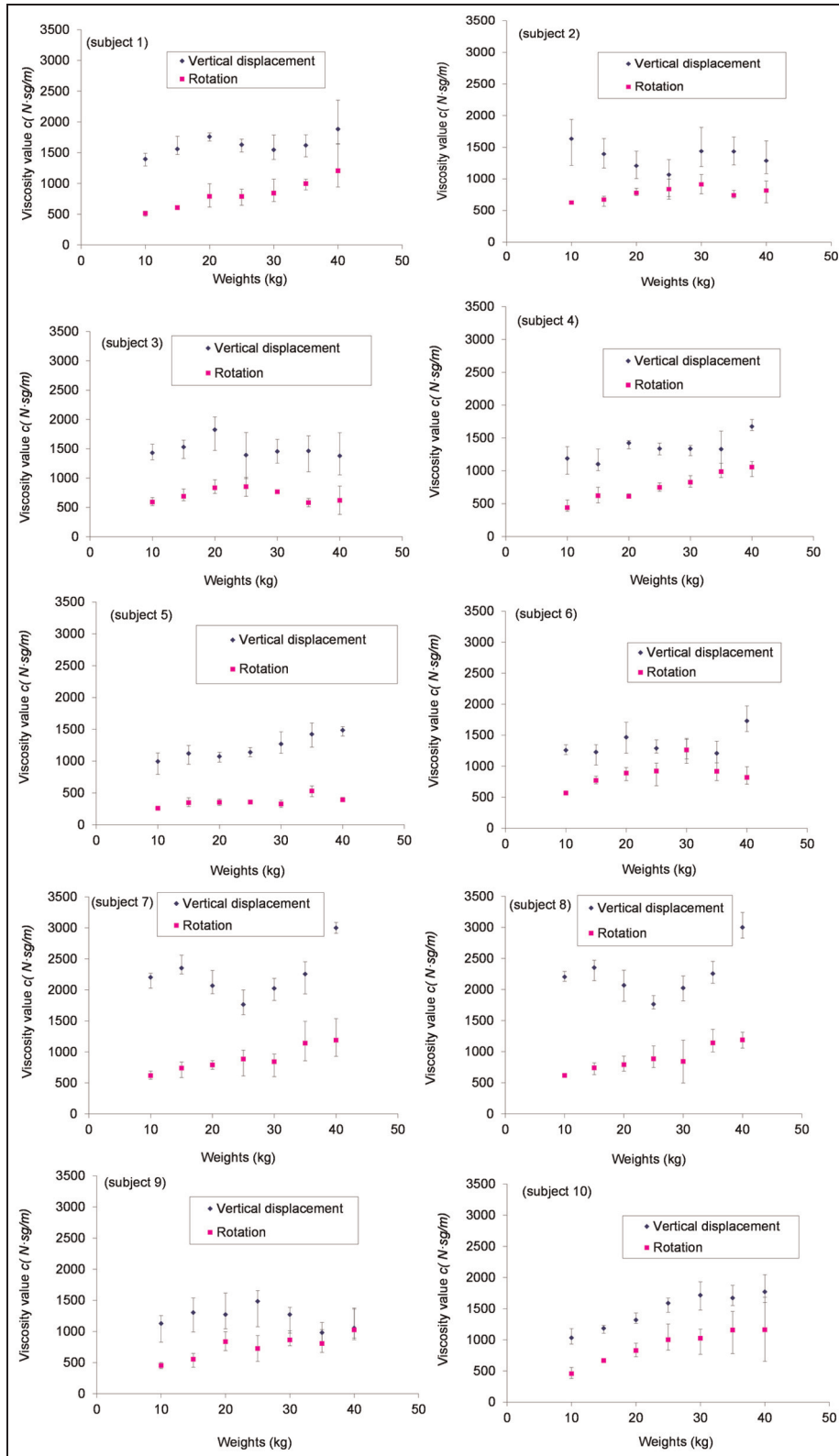


Figure 15. Variation of the apparent viscosity of TS complex with respect to the nominal applied load for the 2 measurement protocols and for the 10 tested subjects.

articulation. For the viscosity values (Table 6), it can be observed that higher dispersion was found within each subject (with CVs up to 28% in the worst case) and also high differences were found between average values for

different subjects. The difference found between both procedures is also remarkable.

While material property values determined from the two measurement protocols analysed in this study were

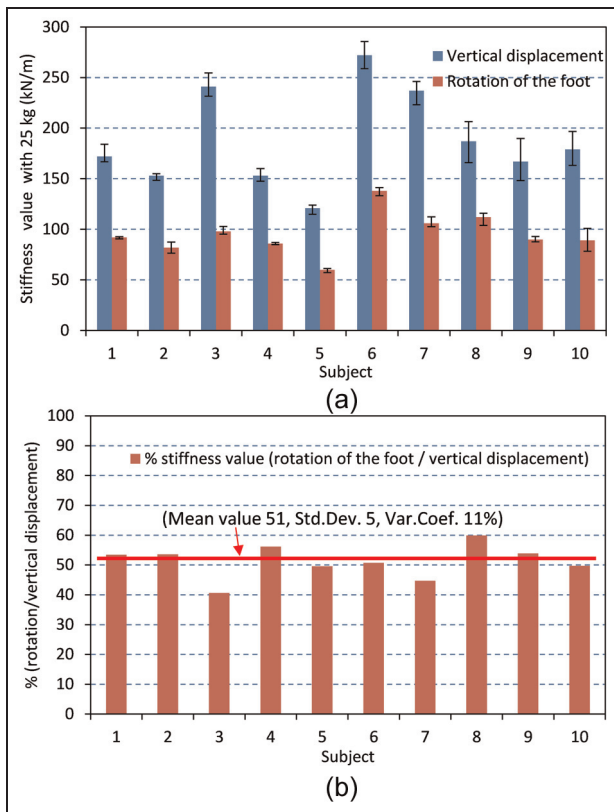


Figure 16. Variation of the apparent viscosity of TS (25 kg of applied load) for the 2 measurement protocols and for the 10 tested subjects: (a) absolute apparent values and (b) relative values.

qualitatively similar, they were not comparable at all from a quantitative point of view. However, this does not mean that the two identification procedures should not be used as independent tools to estimate visco-elastic parameters of the TS MTC for a particular person.

Although in contrast with the literature data (e.g. visco-elastic properties of the human TS quoted in the previous studies^{12,13} agree also in quantitative terms), the results of this study sound logical. The differences seen between the two measurement procedures must derive from two reasons. First, the oscillating mass involved in the two load cases (for a nominal value of M_{tr}) is not the same: this affects the response of the MTC and hence the apparent stiffness of the vibrating system. The stiffness of the muscle depends on the force that it is executing, that is, the pre-stress of the muscle before the movement and this obviously depends (besides the individual and his physical state) on the specific position, weight applied, etc. Second, the two measurement protocols rely on a different theoretical foundation: the first procedure considered the vertical translation of the lower leg, while the second procedure considered the rotation of the foot around the ankle articulation. This led to have different elements participating in the system response thus altering the vibration frequency, which is the basic quantity on which values of mechanical properties depend. In this context, it is noticeable to think of about differences of the common assumption, $M_s \approx M$, made in both procedures.

Table 5. Results obtained for the TS equivalent stiffness (k) for the tested subjects (with 25 kg).

25 kg Subject	Stiffness k (kN/m) for each test				Statistics		
	T1	T2	T3	T4	Mean	SD	CV (%)
TS stiffness using first procedure (vertical displacement)							
S1	166	170	184	166	171.5	8.5	5.0
S2	148	154	155	154	152.8	3.2	2.1
S3	231	232	245	254	240.5	11.0	4.6
S4	149	160	147	154	152.5	5.8	3.8
S5	122	124	124	115	121.3	4.3	3.5
S6	259	273	285	271	272.0	10.6	3.9
S7	239	223	240	246	237.0	9.8	4.1
S8	200	175	166	206	186.8	19.3	10.3
S9	156	190	174	148	167.0	18.8	11.3
S10	166	163	197	190	179.0	17.0	9.5
Total					188.0	47.1	25.1
TS stiffness using second procedure (rotation of the foot)							
S1	92	92	91	93	92.0	0.8	0.9
S2	83	76	81	87	81.8	4.6	5.6
S3	96	95	98	103	98.0	3.6	3.6
S4	87	85	87	84	85.8	1.5	1.7
S5	57	61	61	60	59.8	1.9	3.2
S6	141	138	140	133	138.0	3.6	2.6
S7	103	106	103	112	106.0	4.2	4.0
S8	116	116	113	104	112.3	5.7	5.1
S9	91	93	88	87	89.8	2.8	3.1
S10	101	88	79	89	89.3	9.0	10.1
Total					95.3	20.7	21.7

TS: triceps surae; SD: standard deviation; CV: coefficient of variation.

Table 6. Results obtained for the TS equivalent viscosity (*c*) for the tested subjects (with 25 kg).

25 kg		Viscosity <i>c</i> (N s/m) for each test				Statistics		
Subject	T1	T2	T3	T4	Mean	SD	CV (%)	
TS viscosity using first procedure (vertical displacement)								
S1	1720	1627	1511	1653	1627.8	87.1	5.4	
S2	1301	976	1306	681	1066.0	299.5	28.1	
S3	991	1418	1381	1777	1391.8	321.4	23.1	
S4	1423	1293	1389	1244	1337.3	83.0	6.2	
S5	1154	1118	1067	1215	1138.5	62.2	5.5	
S6	1243	1427	1212	1271	1288.3	95.6	7.4	
S7	1482	2002	1722	1848	1763.5	219.8	12.5	
S8	813	880	1212	1005	977.5	175.4	17.9	
S9	1077	1638	1656	1562	1483.3	273.9	18.5	
S10	1635	1670	1441	1602	1587.0	101.2	6.4	
Total					1366.1	255.9	18.7	
Triceps surae viscosity using second procedure (rotation of the foot)								
S1	644	906	767	834	787.8	111.4	14.1	
S2	835	722	801	997	838.8	115.6	13.8	
S3	903	1011	806	689	852.3	137.3	16.1	
S4	817	719	687	767	747.5	56.8	7.6	
S5	338	366	332	390	356.5	26.8	7.5	
S6	1051	956	999	686	923.0	162.7	17.6	
S7	1026	916	613	983	884.5	186.6	21.1	
S8	504	824	662	475	616.3	161.0	26.1	
S9	717	934	519	734	726.0	169.6	23.4	
S10	1252	1018	836	895	1000.3	184.2	18.4	
Total					773.3	182.1	23.5	

TS: triceps surae; SD: standard deviation; CV: coefficient of variation.

Thus, while in the first procedure the acceleration of all points involved in the movement is basically the same, in the second procedure the acceleration of each point is a function of the distance to the rotation point. All this assigns to the hypothesis made a different level of representativity in each procedure.

Conclusions

This article compared two procedures for evaluating in vivo apparent mechanical properties (stiffness and viscosity) of the TS MTC. Experimental measurements, based on the free vibration technique, were conducted using two experimental set-ups specifically designed. The values of TS visco-elastic parameters were then determined by means of a least-square fitting approach.

In addition to the design and performance of two devices for measuring TS properties, three main contributions can be highlighted. First, a protocol has been proposed and validated to prove the repeatability of the results for a subject under similar testing conditions. Second, a precise procedure of measurement of the lever arms of the foot has been developed and applied to the subjects studied. Finally, a clarification of the presence of a static mass and a dynamic mass appearing in the experiments (distinction omitted in the previous studies) has been carried out.

A good agreement between the experimental data measured by a load cell and the theoretical predictions

provided by an equivalent 1-degree-of-freedom model simulating the dynamic behaviour of the vibrating system was found for both testing protocols. This confirms the feasibility of using the identification procedure developed in this study for many purposes such as to compare characteristics of different subjects or, for a single individual, to control the evolution of MTC properties with respect to time, training and so on.

However, the values of visco-elastic parameters found by considering the vertical displacement of the lower leg or the rotation of the foot around the ankle articulation could be compared with each other only in qualitative terms. The differences in the measurements obtained using both protocols showed a very convincing consistency. This finding is very important if one considers that in this study the same population was submitted to both load cases. Conversely, literature data that indicated also a quantitative correspondence of visco-elastic properties were obtained by considering completely different populations.

Funding

This study was funded by the Junta de Andalucía and Fondo Social Europeo through the Project P08-TEP-04071.

Declaration of conflicting interests

The authors declare that there is no conflict of interest.

References

1. Shorten MR. Muscle elasticity and human performance. In: Van Gheluwe B and Atha J (eds) *Current research in sports biomechanics*. Basel: Karger, 1987, pp.1–18.
2. Horita T, Komi PV, Härmäläinen I, et al. Exhausting stretch-shortening cycle (SSC) exercise causes greater impairment in SSC performance than in pure concentric performance. *Eur J Appl Physiol* 2003; 88: 527–534.
3. Komi PV. Training of muscle strength and power: interaction of neuromotoric, hypertrophic and mechanical factors. *Int J Sports Med* 1986; 7(Suppl.): 10–15.
4. Józsa LG and Kannus P. *Human tendons: anatomy, physiology and pathology*. Champaign, IL: Human Kinetics, 1997.
5. Huxley AF and Simmons RM. Proposed mechanism of force generation in striated muscle. *Nature* 1971; 233: 533–538.
6. Morgan DL. Separation of active and passive components of short-range stiffness of muscle. *Am J Physiol* 1977; 232(1): C45–C49.
7. Rack PM and Westbury DR. Elastic properties of the cat soleus tendon and their functional importance. *J Physiol* 1984; 347: 479–495.
8. Pousson M, Hoecke JV and Goubel F. Changes in elastic characteristics of human muscle induced by eccentric exercise. *J Biomech* 1990; 23(4): 343–348.
9. Fukashiro S, Komi PV, Jarvinen M, et al. In vivo Achilles tendon loading during jumping in humans. *Eur J Appl Physiol* 1995; 71(5): 453–458.
10. Fukashiro S, Itoh M, Ichinose Y, et al. Ultrasonography gives directly but noninvasively elastic characteristic of human tendon in vivo. *Eur J Appl Physiol* 1995; 71(6): 555–557.
11. Lafortune MA, Hennig EM and Lake MJ. Dominant role of interface over knee angle for cushioning impact loading and regulating initial leg stiffness. *J Biomech* 1996; 29(12): 1523–1529.
12. Fukashiro S, Noda M and Shibayama A. In vivo determination of muscle viscoelasticity in the human leg. *Acta Physiol Scand* 2001; 172(4): 241–248.
13. Babic J and Lenarcic J. In vivo determination of triceps surae muscle–tendon complex viscoelastic properties. *Eur J Appl Physiol* 2004; 92(4–5): 477–484.
14. Faria A, Gabriel R, Abrantes J, et al. Triceps-surae musculotendinous stiffness: relative differences between obese and non-obese postmenopausal women. *Clin Biomech* 2010; 24: 866–871.
15. Hill AV. The heat of shortening and the dynamic constants of muscle. *P Roy Soc Lond B Bio* 1938; 126(843): 136–195.
16. Zatsiorsky V and Seluyanov V. The mass and inertial characteristics of the main segments of the human body. In: Matsui H and Kobayahi K (eds) *Biomechanics VIII-B*. Champaign, IL: Human Kinetics, 1983, pp.1152–1159.
17. Zatsiorsky VM, Seluyanov VN and Chugunova L. In vivo body segment inertial parameters determination using a gamma-scanner method. In: Berme N and Cappozzo A (eds) *Biomechanics of human movement: application in rehabilitation, sports, and ergonomics*. Worthington, OH: Bertec Corporation, 1990, pp.187–202.
18. Donahue TLH, Hull ML, Rashid MM, et al. A finite element model of the human knee joint for the study of tibio-femoral contact. *J Biomech Eng* 2000; 124: 273–280.
19. Strickland MA and Taylor M. In-silico wear prediction for knee replacements – methodology and corroboration. *J Biomech* 2009; 42: 1469–1474.
20. París-García F. *In-vivo determination of the viscoelastic properties of the triceps surae by means of the free vibration technique*. PhD Thesis, University of Seville, Spain, 2010 (in Spanish).
21. Clough RW and Penzien J. *Dynamics of structures*. New York: McGraw-Hill, 1975.